

## Structural studies of thin Pd films loaded with hydrogen

O Melikhova<sup>1</sup>, J Čížek<sup>1</sup>, M Vlček<sup>1</sup>, F Lukáč<sup>1</sup>, I Procházka<sup>1</sup>,  
W Anwand<sup>2</sup>, G Brauer<sup>2</sup>

<sup>1</sup>Charles University in Prague, Faculty of Mathematics and Physics,  
V Holešovičkách 2, 180 00 Prague 8, Czech Republic

<sup>2</sup>Institut für Strahlenphysik, Helmholtz-Zentrum Dresden-Rossendorf,  
Postfach 510119, D-01314, Dresden, Germany

E-mail: oksivmel@yahoo.com

**Abstract.** In this work variable energy positron annihilation spectroscopy was employed for investigation of defects created in Pd films electrochemically charged with hydrogen. The development of hydrogen-induced defects in nanocrystalline, polycrystalline and epitaxial Pd films were compared. It was found that absorbed hydrogen causes plastic deformation and increases defect density in all Pd films studied. Moreover, buckling was observed in nanocrystalline and polycrystalline films loaded above certain critical hydrogen concentration.

### 1. Introduction

Pd is a very important material for hydrogen technologies and is also used as a model system for study of hydrogen behaviour in metal lattice. In a perfect Pd lattice hydrogen occupies octahedral interstitial sites and causes remarkable volume expansion [1]. Hydrogen strongly interacts with defects: it can be trapped at open volumes defects like vacancies, dislocations and grain boundaries (GBs) and may also introduce new defects [2]. In this work we employed variable energy slow positron spectroscopy (VEPAS) to study the hydrogen interaction with defects in Pd films with various microstructures ranging from epitaxial to nanocrystalline.

### 2. Experimental Details

Three kinds of Pd films were deposited by cold cathode beam sputtering on (11-20) sapphire substrates: (i) nanocrystalline films deposited at room temperature; (ii) polycrystalline films deposited at room temperature and then annealed in vacuum at 800°C for 1h; (iii) epitaxial films deposited at 800°C. The thickness of the deposited films determined by stylus profilometry was  $(1080 \pm 10)$  nm and  $(1040 \pm 10)$  nm for the nanocrystalline and the polycrystalline film, respectively, and  $(485 \pm 5)$  nm for the epitaxial film. Scanning electron microscopy and X-ray diffraction [3] revealed that films deposited at room temperature exhibit a nanocrystalline structure consisting of column-like crystallites with the mean width of  $\approx 50$  nm; subsequent annealing at 800°C led to a pronounced grain growth and the annealed films exhibit polycrystalline structure with the grain size of  $\approx 2.5$   $\mu\text{m}$ . The films deposited at 800°C are single crystals with well defined orientation with respect to the sapphire substrate.

Hydrogen loading was performed electrochemically by constant current pulses in a galvanic cell filled with a mixture of  $\text{H}_3\text{PO}_4$  and glycerine (1:2). The hydrogen concentration  $x_H$  introduced into the sample was calculated from the transported charge using the Faraday's law. Hydrogen loading introduces large stresses since the films are fixed on a substrate which prevents in-plane expansion [3].



VEPAS studies were performed on a slow positron beam SPONSOR [4] with positron energy adjustable from 0.03 to 36 keV. Doppler broadening of the annihilation line was measured by a HPGe detector with energy resolution of 1.09 keV at 511 keV and evaluated using the  $S$  and  $W$  parameters. All  $S$  and  $W$  parameters were normalized to bulk values  $S_0$ ,  $W_0$  measured in a well annealed bulk Pd.

**Table 1.** Dislocation densities estimated from VEPAS results by Eq. (1).

sample	virgin state		H-loaded up to $x_H = 1.0$	
	$L_+$ (nm)	$\rho_D$ (m <sup>-2</sup> )	$L_+$ (nm)	$\rho_D$ (m <sup>-2</sup> )
bulk Pd cold rolled	$49 \pm 2$	$(7.6 \pm 0.6) \times 10^{14}$	-	-
polycrystalline Pd film	$106 \pm 1$	$(9.2 \pm 0.4) \times 10^{13}$	$66 \pm 3$	$(3.8 \pm 0.8) \times 10^{14}$
epitaxial Pd film	$16 \pm 2$	$(8 \pm 1) \times 10^{15}$	$2.3 \pm 0.8$	$(4 \pm 1) \times 10^{16}$

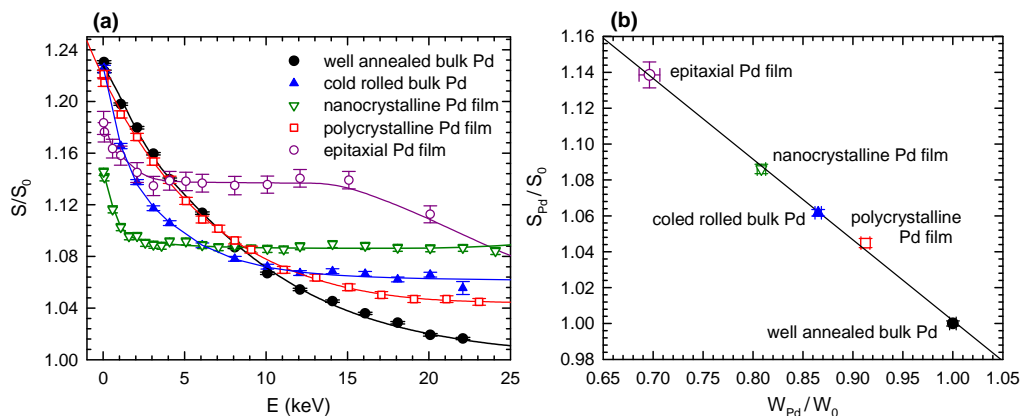


**Figure 1.** (a)  $S(E)$  curves for the virgin films and well annealed and cold rolled bulk Pd. Solid lines show model curves calculated by VEPFIT; (b)  $S$ - $W$  plot constructed from bulk values.

### 3. Results and Discussion

Fig. 1 shows the dependences of  $S$  on the positron energy  $E$  for the virgin films. At very low energies virtually all positrons are annihilated at the surface. With increasing energy positrons penetrate deeper and deeper into the sample and the fraction of positrons diffusing back to the surface decreases. This is reflected by a decrease of  $S$  from a surface value down to a bulk value. Note that in the epitaxial film with lower thickness positrons penetrate into the substrate at  $E > 15$  keV which leads to a further decrease of  $S$ . The  $S(E)$  curves were fitted by VEPFIT [5] and the calculated model curves plotted in Fig. 1 by solid lines describe the experimental points accurately.

The  $S(E)$  curves for a well annealed (1000°C/1h) and cold rolled (thickness reduction of 50%) bulk Pd are plotted in Fig. 1 as well. Positron lifetime measurement confirmed that the well annealed bulk Pd exhibits a single component spectrum with the lifetime  $\tau_B = (111 \pm 1)$  ps which agrees well with the calculated lifetime of free positrons in a perfect Pd crystal [6]. Hence, the well annealed bulk Pd can be considered as a defect-free material. Indeed, the positron diffusion length  $L_{+,B} = (151 \pm 4)$  nm obtained from fitting of the  $S(E)$  curve of this sample falls into the range expected for perfect (defect-free) metals. The cold rolled bulk Pd sample exhibits shorter positron diffusion length  $L_+ = (49 \pm 2)$  nm and higher bulk  $S$  parameter due to positron trapping at dislocations introduced by plastic deformation. The nanocrystalline film exhibits even shorter positron diffusion length  $L_+ = (41 \pm 5)$  nm and higher  $S$  parameter than the cold rolled bulk Pd. This is not surprising since the average width of nanocrystalline columns is shorter than  $L_{+,B}$  and majority of positrons, thereby, diffuse to GBs and are trapped at open volume defects there. Annealing of the film at 800°C led to a decrease of  $S$  and an increase of  $L_+$  due to intensive grain growth which substantially reduced the volume fraction of GBs.

The epitaxial film exhibits the highest  $S$  and the shortest  $L_+$  among the samples studied. This is likely due to a dense network of misfit dislocations induced by relatively large lattice mismatch ( $\sim 30\%$ ) between the Pd films and the substrate. Note that low angle GBs can be formed in the film by accumulation of misfit dislocations to compensate for the misfit. In VEPAS study low angle GBs cannot be distinguished from isolated misfit dislocations but since XRD characterization of the epitaxial film [3] showed very sharp rocking curve one can conclude that although formation of low angle GBs cannot be excluded they do not represent dominant kind of defects in the sample.

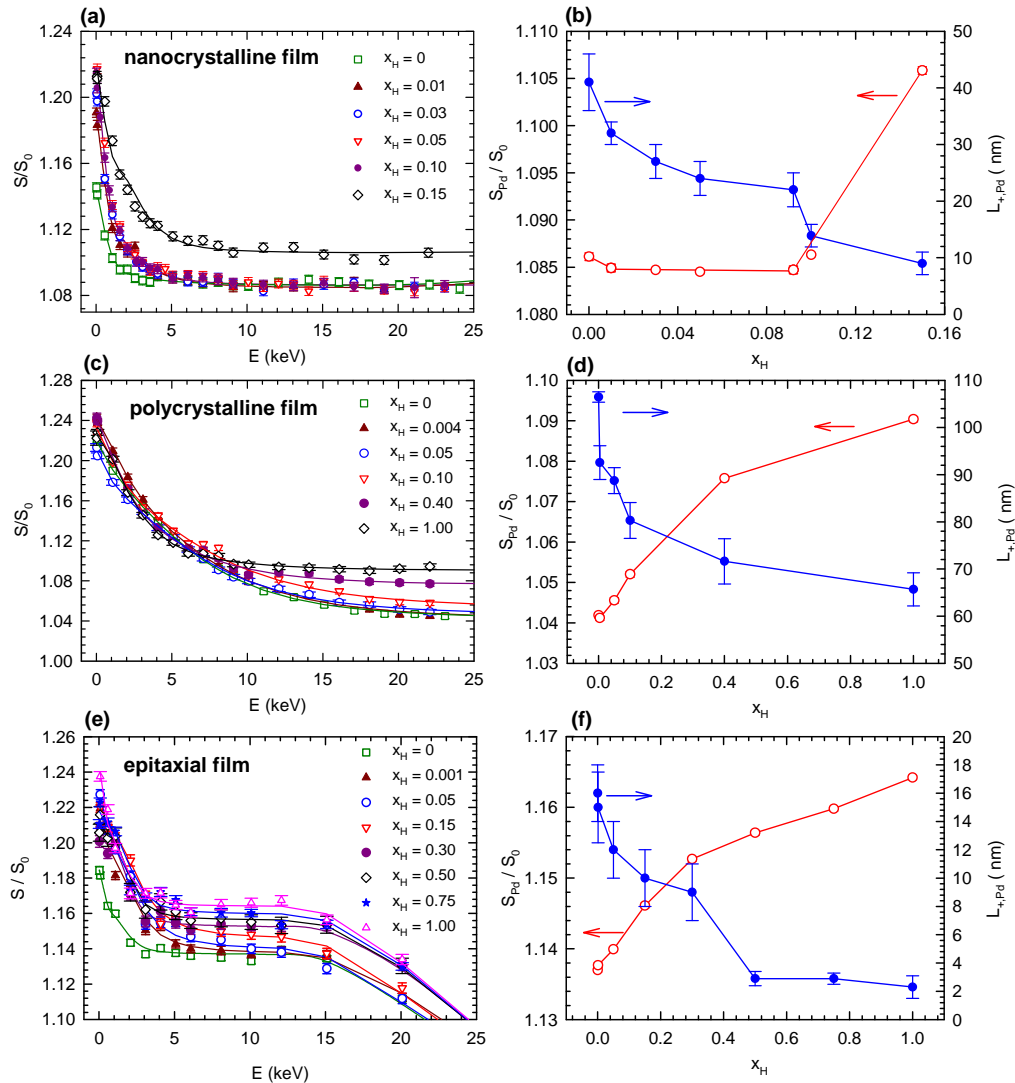


**Figure 2.** Left panels: dependence of the  $S$  parameter on the energy of incident positrons for (a) nanocrystalline, (c) polycrystalline and (e) epitaxial film. Solid lines show model curves calculated by VEPFIT. Right panels: dependence of the bulk  $S$  parameter and positron diffusion length on the hydrogen concentration for (b) nanocrystalline, (d) polycrystalline and (f) epitaxial film.

Although a dislocation line itself is a shallow positron trap a positron trapped there quickly diffuses along the dislocation and is finally trapped at vacancies associated with jogs or anchored in the compressive elastic field of dislocation. Hence, positrons trapped at dislocations are finally annihilated at vacancy-like defects. It is known [7] that positrons trapped at GBs exhibit lifetime comparable to a vacancy. Thus, in all Pd samples studied positrons are confined in similar kind of defects characterized by open volume comparable to a monovacancy. This is confirmed by  $S$ - $W$  plot constructed from the

bulk values and plotted in Fig. 1b. Since all points fall on a straight line connecting the well annealed bulk sample and the epitaxial film positrons are annihilated at similar kind of defects but defect density in the samples differs. Table 1 shows the density of dislocations estimated from the expression

$$\rho_D = \frac{1}{v_D \tau_B} \left( \frac{L_+^2}{L_{+,B}^2} - 1 \right), \quad (1)$$

where  $v_D \approx 10^{-4} \text{ m}^2\text{s}^{-1}$  is the specific positron trapping rate for dislocations [8]. Note that Eq. (1) is not applicable for the nanocrystalline film where positrons are trapped predominantly at GBs.

The films were subsequently step-by-step loaded with hydrogen. Left panels in Fig. 2 show the  $S(E)$  curves obtained for nanocrystalline, polycrystalline and epitaxial films, respectively. The bulk  $S$  parameter and positron diffusion length obtained from fitting are plotted in the right panels as a function of hydrogen concentration  $x_H$ . In the polycrystalline and the epitaxial film  $S$  increases with  $x_H$  while  $L_+$  decreases testifying to formation of new defects introduced by hydrogen loading. It indicates that stresses induced by absorbed hydrogen lead to plastic deformation which creates dislocations in the films. On the other hand, in the nanocrystalline film  $S$  firstly decreases because hydrogen fills open volume defects at GBs. At hydrogen concentrations  $x_H > 0.02$  all available deep traps at GBs are already filled and  $S$  remains approximately constant. When hydrogen concentration exceeds  $x_H \approx 0.1$  hydrogen-induced plastic deformation takes place and creates dislocations in the film. Hence dislocation density in hydrogen loaded films increased remarkably. This can be seen in Table 1 containing dislocation densities in the hydrogen loaded films estimated by Eq. (1). Moreover at  $x_H > 0.1$  hydrogen-induced stresses in the nanocrystalline film exceeded film adhesion to substrate and buckling of the film occurs. Delamination of the film starts at edges but finally at  $x_H > 0.15$  the whole film is detached from the substrate (VEPAS measurement was stopped at that point). Annealing at  $800^\circ\text{C}$  improved film bonding to the substrate and the onset of buckling was shifted to  $x_H > 0.3$ . In the epitaxial film no buckles were formed during the whole loading procedure, i.e. up to  $x_H \approx 1$ . Buckling is always accompanied by plastic deformation as was confirmed also by acoustic emission [9].

#### 4. Conclusions

Hydrogen interaction with defects in Pd films was studied. It was found that hydrogen is trapped at open volume misfit defects at grain boundaries. Moreover, absorbed hydrogen introduces high stresses which inevitably lead to plastic deformation and introduces a high number of dislocations into the film. When the stresses exceed the film adhesion to the substrate buckling of the film occurs.

#### Acknowledgements

Financial support from the Ministry of Education, Youths and Sports of the Czech Republic (project LH12173) and the Czech Science Foundation (project P108-13-09436S) are highly acknowledged.

#### 5. References

- [1] Flanagan T B, Oates W A 1991 *Annu. Rev. Mater. Sci.* **21**, p. 269
- [2] Pundt A, Kirchheim R 2006 *Annu. Rev. Mater. Res.* **36**, p. 555
- [3] Čížek J, Melikhova O, Vlček M, Lukáč F, Vlach M, Procházka I, Anwand W, Brauer G, Mücklich A, Wagner S, Uchida H, Pundt A 2013, *Int. J. Hydrogen Energy* **38**, p. 12115
- [4] Anwand W, Brauer G, Butterling M, Kissenger H-R, Wagner A 2012 *Defect and Diffusion Forum* **331**, p. 25
- [5] van Veen A, Schut H, Clement M, de Nijs J, Kruseman A, Ijpma M 1995 *Appl. Surf. Sci.* **85**, 216
- [6] Campillo Robles J M, Ogando E, Plazaola F 2007, *J. Phys.: Condens. Matter* **19**, 176222
- [7] Dupasquier A, Romero R, Somoza A 1993, *Phys. Rev. B* **48**, p. 9235
- [8] Hautojärvi P, Corbel C 1995 *Proceedings of the International School of Physics "Enrico Fermi"*, Course CXXV ed A Dupasquier, A P Mills (Varena: IOS Press) pp 491
- [9] Čížek J, Procházka I, Vlach M, Žaludová N, Daniš S, Dobroň P, Chmelík F, Brauer G, Anwand W, Mücklich A, Nikitin E, Gemma R, Kirchheim R, Pundt A, 2008 *Appl. Surf. Sci.* **255**, p. 241